JOURNAL OF MATERIALS SCIENCE 10 (1975) 2062–2070

Tensile failure mechanisms in carbon fibre reinforced plastics

M. FUWA*, A. R. BUNSELL†, B. HARRIS
School of Applied Sciences, University of Sussex, Falmer, Brighton, UK

Tensile failure mechanisms in type I carbon fibre-reinforced epoxy resin have been studied by examining the modes of failure of cured and semi-cured CFRP and of fibre bundle specimens. The rigid matrix in the cured material modified the appearance of the fractured specimen but by detecting the acoustic emission generated during loading the basic fibre bundle behaviour was found to exert a major influence on fracture. Microscopic examination of fractured CFRP specimens has revealed that consecutive fibre failure may be restricted to sub-bundles as a result of shearing between these sub-bundles, and that the material is weakened by a number of internal failures that are not necessarily connected. Ultimate failure seems to be statistically determined and it is a characteristic of the material that some scatter in the strength of CFRP must be expected.

1. Introduction

Full appreciation of the mechanical behaviour of components made of carbon fibre-reinforced plastic (CFRP) will not be achieved until the failure mechanism in this material is better understood. For while such traditional approaches to characterising the mechanical properties of materials as the use of linear elastic fracture mechanics may be useful in establishing design criteria, the fundamental fracture behaviour of CFRP may be totally different from that which the application of such design techniques predicates.

The assumption that CFRP and other fibre-reinforced materials may be treated as anisotropic but homogeneous materials has been made by some workers [1–4], while others have tackled the problem from a microscopic point of view, considering mechanisms relating to single fibres and fibre bundles [5–7]. The latter argue that final failure of a fibre-reinforced material is due to an accumulation of fibre breaks which are not necessarily originally connected or related. Eventual failure is considered to occur when a particular cross-section is so weakened as to be unable to support the applied load. The former approach implies failure after progressive crack growth through the material originating from one critical flaw.

Optical microscope and other "metallographic" techniques of studying mechanisms of failure in materials are largely ineffective with black, opaque CFRP containing many thousands of carbon fibres only 7 μm in diameter. In this study we have used an acoustic emission (AE) technique to monitor the deformation processes which occur in CFRP specimens under stress and the interpretation of AE patterns together with the appropriate stress–strain curves has suggested a clearer picture of the mechanisms involved.

2. Acoustic emission

The occurrence of local damage such as fibre failure, fibre/matrix debonding, and matrix cracking in CFRP can be expected to generate bursts of vibrations which travel through the material and which can be detected by suitably sensitive transducers coupled to the surface. The intensity of these acoustic emissions (or stress-wave emissions), which is proportional to the total energy involved in the original process, can be used to obtain an insight into mechanisms

* Present address: Mitsubishi Petrochemical Company, Ibarati, Japan.
† Present address: Centre des Matériaux, Ecole Nationale Supérieure des Mines de Paris, Carbeille, Essonnes, France.

occurring within the specimen. The AE equipment used in our work was a Dunegan Research Corp. system comprising their S/D-60 pre-amplifier with a model 3000 amplifier and counter. The apparatus was used to obtain either a cumulative count of emissions (total number of counts during a test) or the rate of emission which was obtained by counting over set periods of time. The transducers were PZT-5 ceramic piezoelectric transducers coupled to the specimens by silicone grease.

An assessment of the value of monitoring acoustic emissions from CFRP under load has already been made and will be presented elsewhere [8].

3. Tensile specimens

In order to avoid ambiguities in the acoustic emission patterns, a simple plane specimen shape was adopted since we had found that the waisting or notching of samples gave rise to additional emissions due to shear failure. The design adopted ensured, as far as possible, that specimens experienced only tensile forces. Aluminium tabs were bonded to the sample ends, as illustrated in Fig. 1, in order to prevent grip damage. The dimensions of the specimens were 40 mm × 10 mm × 0.35 mm and the unidirectionally aligned fibres were parallel with the long direction.

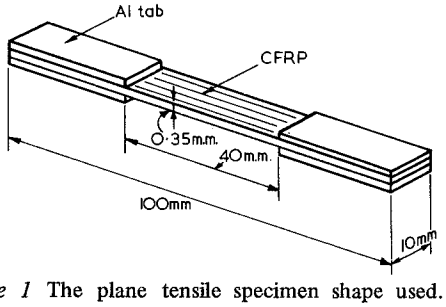

Figure 1 The plane tensile specimen shape used. The aluminium tabs bonded to the ends of the unidirectional CFRP provide regions for gripping.

Three types of sample have been tested, all containing type 1 continuous carbon fibre. The first was a fully-cured, carbon fibre epoxy composite prepared from Ciba-Geigy 905C resin pre-impregnated sheet, with a fibre volume fraction of 0.35. The second type was the same material with the resin in semi-cured form, and the third type consisted of fibre bundles containing no resin. The latter were obtained by dissolving the resin away from the pre-impregnated sheet. The fully-cured samples were made by hot pressing single pre-impregnated sheets at 1.5 MN m^{-2} for 1 h at 180° C, after which they were allowed to cool down to room temperature. The semi-cured material was made in a similar manner, but during heating the gauge length of the specimen was continuously sprayed with water. The finished test pieces retained much of the flexibility of the original pre-preg over their gauge length but the regions bonded to the aluminium tabs were fully cured and rigid. This semi-cured material was also used to make the fibre bundle specimens, the gauge length of the samples being dipped into hot sulphuric acid for 50 min in order to remove the resin matrix completely. A comparison of the properties and appearance of fibres before and after exposure to hot sulphuric acid showed that the acid did not affect the fibres. By preparing the three types of samples in this way from the same pre-preg sheets we were able to ensure that the same degree of alignment and the same number of fibres were to be found in all of the specimens, and that the mechanical characteristics of the bundles were the same as those in the samples containing resin.

The fibre volume fraction of our materials was determined gravimetrically, the matrix being removed by acid digestion as described above. Any excess acid remaining on the fibres was neutralized with hydrogen peroxide solution before the specimens were washed in alcohol and dried. In this way the scatter in the strengths of samples due to variations in fibre volume fraction was eliminated by normalizing to a volume fraction of 0.35.

4. Tensile tests

All tests were conducted in an Instron at a cross-head speed of 0.05 mm min^{-1}. Seven series of ten tests each were carried out on fully-cured CFRP, and one series each of seven tests was carried out on semi-cured and bundle specimens.

The measured tensile strengths of these materials are recorded in Table I and are plotted against fibre volume fraction in Fig. 2. Here they can be compared with the band of strengths, indicated by dotted lines, predicted by the mixture rule from the upper and lower strength limits for type 1 carbon fibre given by Courtaulds [9]. The yield strength of epoxy resin is taken as 50 MN m^{-2}.

The high coefficients of variation show that there is considerable scatter in tensile strength even when specimens are cut from the same plate and the results are normalized to account for the

TABLE I Tensile test results for cured and semi-cured CFRP and bundles of type 1 carbon fibre

Test series	Number of specimens	Mean tensile strength ($MN\,m^{-2}$)	Standard deviation ($MN\,m^{-2}$)	Coefficient of variation (%)	Range of fibre volume fraction (%)
Cured A	10	610	76	12.5	30–37
B	6	730	54	7.4	30–40
C	3	880	62	7.0	37–42
D	6	600	102	17.1	30–37
E	10	770	117	15.1	33–42
F	9	680	58	8.6	37–42
G	7	880	168	19.1	37–42
Semi-cured H	7	690	17	2.5	–
Bundle I	7	590	17	2.9	–

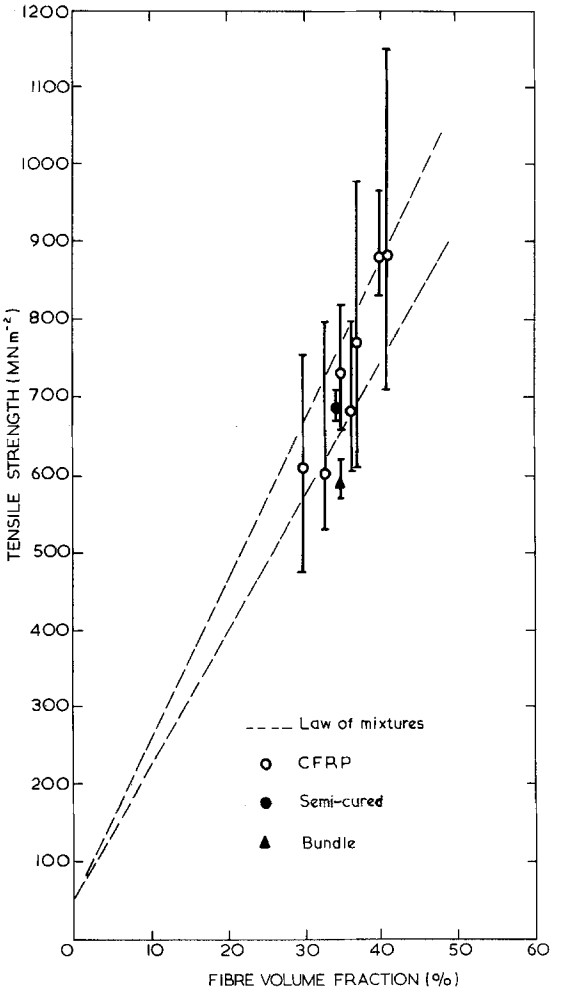

Figure 2 Tensile strengths against fibre volume fraction for the cured and semi-cured CFRP and bundles of type 1 carbon fibre used in this study.

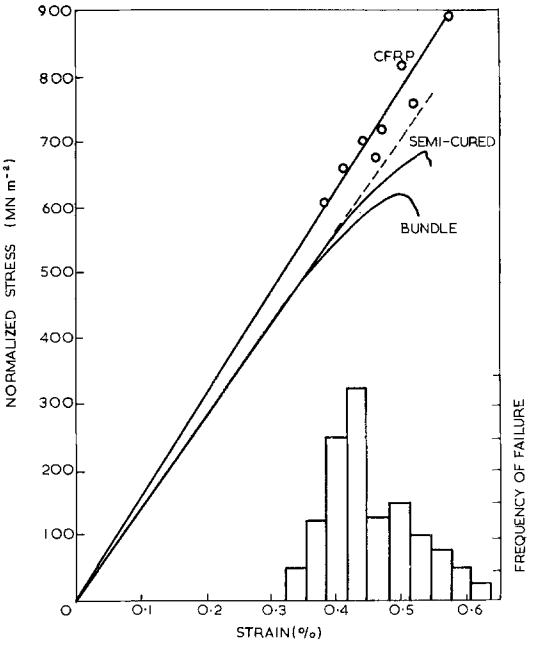

Figure 3 Typical stress–strain curves of cured and semi-cured CFRP and bundles of type 1 carbon fibre. The histogram inset into the figure shows the frequency distribution of the failure strains of all the cured CFRP specimens tested.

variation in fibre volume fraction, as has been done in Table I. This suggests that at least part of the variability may be an inherent characteristic of the material. The coefficients of variation of fibre bundle and semi-cured specimens were found to be smaller than that of the fully-cured composite.

The stress–strain curves of the cured CFRP specimens were found to be almost linear with an abrupt brittle failure as shown in Fig. 3. The mean value of Young's modulus was $155\,GN\,m^{-2}$ with a coefficient of variation of 3.6% and maximum and minimum values of 164 and $147\,GN\,m^{-2}$. Also shown in Fig. 3 are typical stress–strain curves for the semi-cured and bundle specimens and it can be seen that the absence of a rigid matrix results in a lower initial modulus. The curves for both types of material are no longer linear and the extent of the deviation is more pronounced in the fibre bundles. Both of these types of sample showed evidence of some slackness in the fibre bundles, their load–

deflection curves being non-linear at very low strains and becoming linear only as the majority of fibres in the bundle took up the strain. The rigid matrix in the cured material inhibits major fibre readjustments and the stress–strain curves for these samples were linear from the origin. This effect of fibre slackness has not been shown in the diagram, the linear portion of the curve having been extrapolated back to zero load. The failure points of cured CFRP specimens from one series of tests are shown as open circles. It is significant that the specimen which failed with the greatest extension had exceeded that strain at which all of the fibres in the bundle had failed, which means that each fibre in the composite must have broken at least once. The histogram inset into Fig. 3 shows the frequency distribution of the failure strains of all CFRP specimens: its peak is at a strain close to that at which the stress–strain curves of both bundles and semi-cured specimens show marked deviations from linearity.

The bundle specimens reached their maximum load carrying capability at a strain of around 0.5% and catastrophic failure occurred before 0.55%. The stress–strain curves of the bundle specimens were linear up to about 0.35% after which the slope of the curve began to decrease, suggesting the occurrence of a significant number of fibre failures. Semi-cured specimens behaved in a similar manner although the decrease in the slope of the stress–strain curve beyond 0.35% strain was smaller and these specimens reached their maximum load carrying ability at a slightly greater strain. Both of these effects can be explained in terms of the partial contribution of the matrix. Catastrophic failure of both semi-cured and bundle specimens occurred at the same strain, about 0.53%. The wide range of failure strains of CFRP specimens is in marked contrast to the quite consistent values for both bundle and semi-cured specimens.

At this point several observations on these results can be made.

(1) The weakest fully-cured specimen failed at a strain of 0.32%, close to the strain at which our results for bundles and semi-cured samples suggest significant numbers of fibre failures will begin to occur.

(2) About 80% of cured specimens failed before the maximum failure strain for bundle specimens.

(3) Some cured specimens survived to strains greater than 0.55% at which level all the fibres in the semi-cured and bundle specimens had broken.

The fact that 60% of fully-cured specimens failed at strains lower than 0.45%, a level at which only an estimated 10% of the fibres in the bundles had failed, suggests that fibres do not fail in isolation but rather that a progressive failure mechanism such as related fibre breakage or crack propagation could be occurring. Alternatively, the observation that some samples failed at strains greater than the bundles were able to sustain suggests that random fibre failure may be occurring throughout the sample and the ultimate failure of the specimens is a statistically-determined occurrence. To investigate these points further we have monitored the acoustic emission given out from the same types of sample during loading.

5. Acoustic emission studies

The emissions generated during the loading of CFRP specimens have been monitored in order to detect damage occurring within the specimen. An amplification gain of up to 80 dB has been used and by limiting the maximum gain to this level we could be sure of excluding from the count any electrical noise inherent in the system. A gain of 80 dB meant that the only signals counted were those greater than a threshold of 0.1 mV at the transducer.

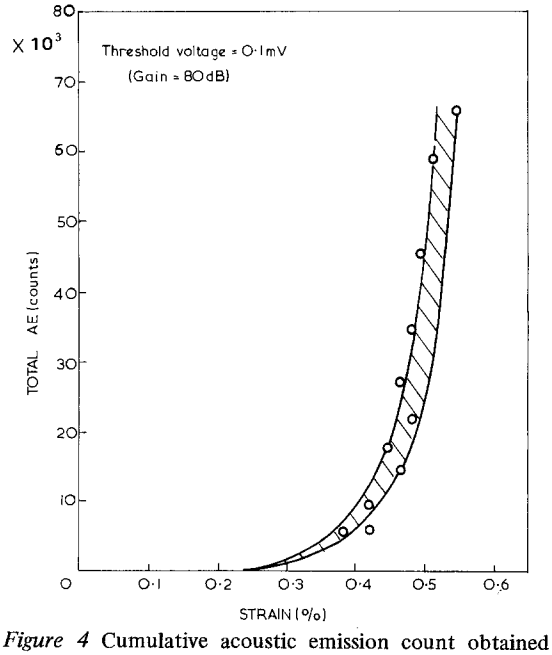

Figure 4 Cumulative acoustic emission count obtained with a gain of 80 dB from a monotonic tensile test of unidirectional CFRP. Data points represent failure of individual samples.

Fig. 4 shows the cumulative AE count pattern obtained with a gain of 80 dB from cured samples of CFRP. The two lines in Fig. 4 show the extent of variation found in the emission pattern. This variation must partly be due to attenuation since fractures occur all over the gauge length and, therefore, at differing distances from the transducer. The AE patterns were all similar to the exponentially increasing trend found by others [10] for CFRP specimens loaded in tension. It is a general feature of these patterns that a sharp increase of emission occurs between 0.35 and 0.4% strain, which coincides with that critical strain for bundle specimens at which significant numbers of fibres fail.

As well as being counted, the acoustic emissions were observed, after amplification, on an oscilloscope so that the effect of using different threshold levels was investigated. The threshold level was varied from 0.1 to 1 mV at the transducer and, as Fig. 5 shows, different numbers of emissions were counted. Both from the counts shown in Fig. 5 and also from the observations of the signals

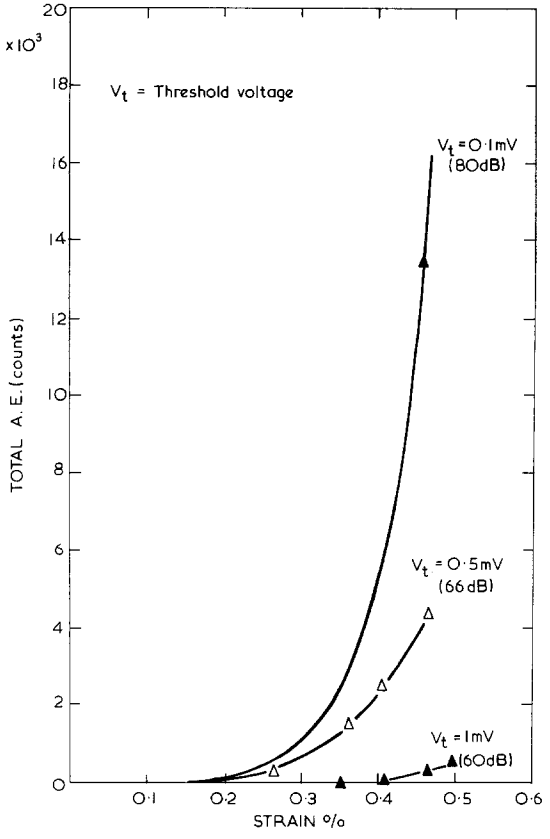

Figure 5 Cumulative acoustic emission count obtained at different gains from monotonic tensile tests of unidirectional CFRP strained to failure.

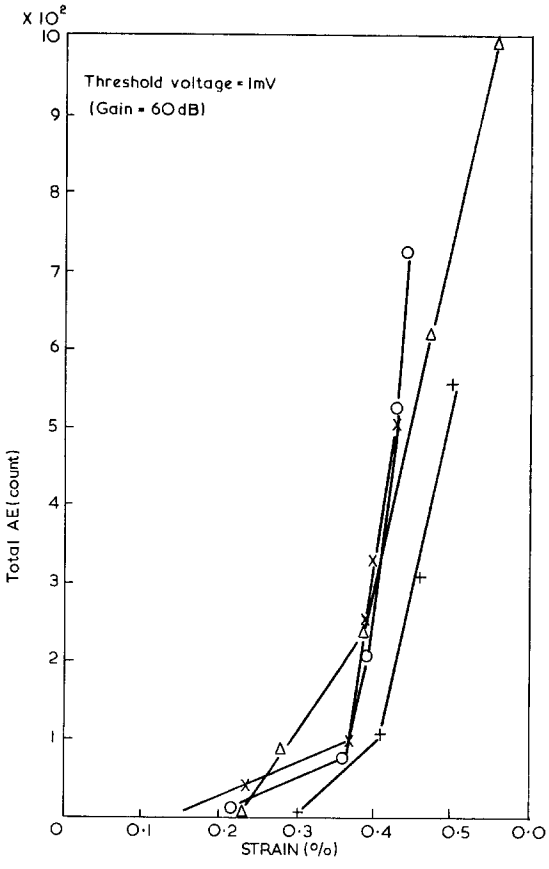

Figure 6 The number of emissions greater than 1 mV can be seen to increase sharply around a strain of 0.35% in a simple tensile test.

shown on the oscilloscope it was clear that the numbers of signals greater than 1 mV began to increase sharply at strains between 0.35 and 0.4%. This is more clearly shown in Fig. 6. The increase in numbers of larger signals was also accompanied by a much larger increase in emissions of 0.1 mV or less, particularly towards the last stage of loading.

A direct comparison of numbers of emissions from cured specimens and from bundle specimens is not possible because of differences in the media through which the emissions reach the transducer. In the case of bundles, emissions reached the transducer only through the silicone grease coupling agent which had penetrated into the bundle but did not contribute to its strength. For this reason the characteristic shape of the acoustic emission pattern, relative to strain, rather than total numbers of counts, was considered to be the more informative method of analysis.

A typical AE pattern for bundle specimens is shown in Fig. 7: the two curves are for gains of 80 and 60 dB. The number of emissions increases

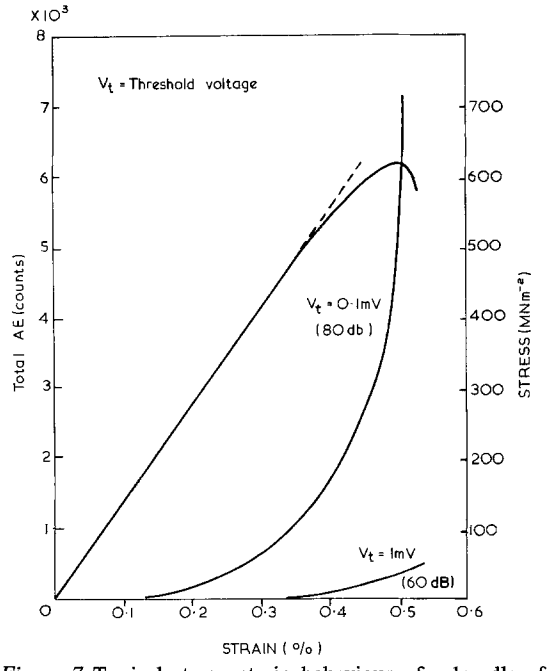

Figure 7 Typical stress–strain behaviour of a bundle of type 1 carbon fibres together with corresponding acoustic emission obtained at two different sensitivities.

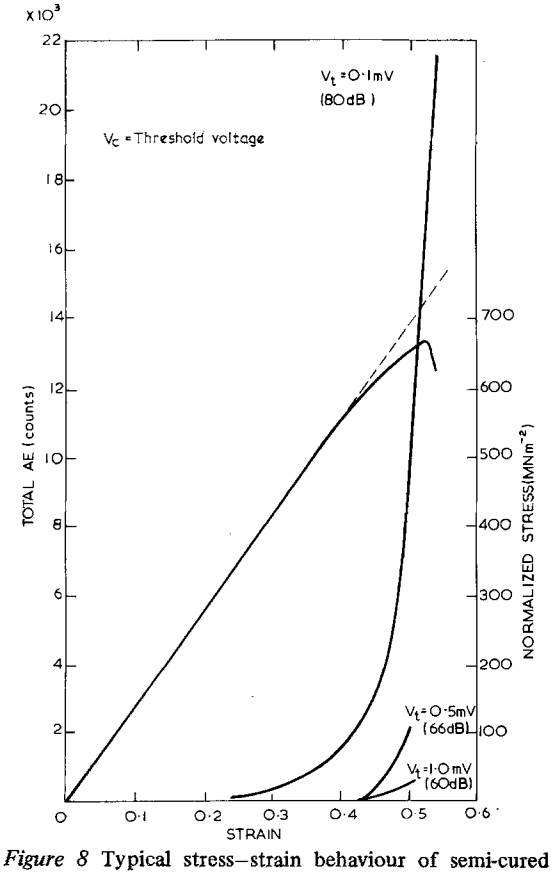

Figure 8 Typical stress–strain behaviour of semi-cured CFRP together with corresponding acoustic emission obtained at three different sensitivities.

gradually from a low strain, but a rapid increase begins from about 0.35% strain at which point the load trace begins to deviate from linearity. This trend of emission from bundles coincides with the observed pattern of behaviour of the cured specimens.

Similar acoustic emission patterns were obtained from semi-cured specimens, as Fig. 8 shows. We note, particularly, that only a few, sporadic emissions were detected during the pulling-out of the fibres from the soft matrix after failure of the specimen and we conclude therefore that most of the emissions recorded were generated by fibre failure alone and not by matrix deformation in these semi-cured specimens.

6. Macroscopic examination

A single fibre loaded to failure is expected to fracture at its weakest point the position of which is determined by the presence of some internal or surface flaw. The fibres in a bundle will, therefore, fail randomly throughout the specimen gauge length and each fibre failure will be independent of the failure of others. The presence of a soft matrix incapable of supporting high shear loads between fibres, such as that in the semi-cured specimens, would not be expected to alter this situation, and Fig. 9 shows that bundle and semi-

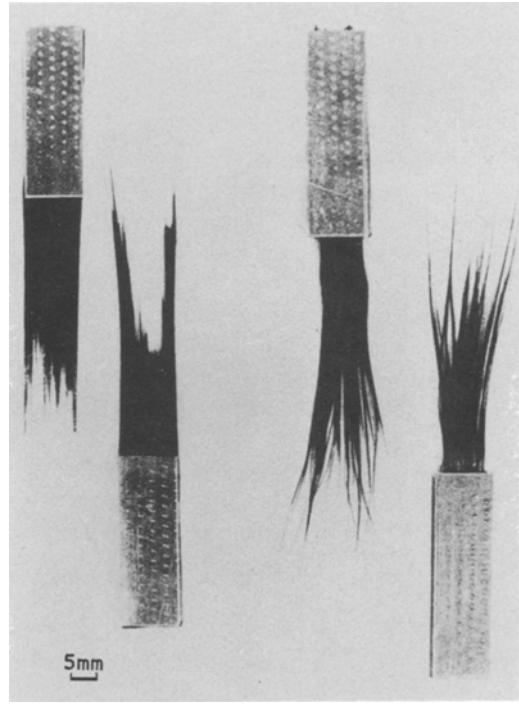

Figure 9 Typical modes of fracture of semi-cured CFRP (left) and bundles of type 1 carbon fibre.

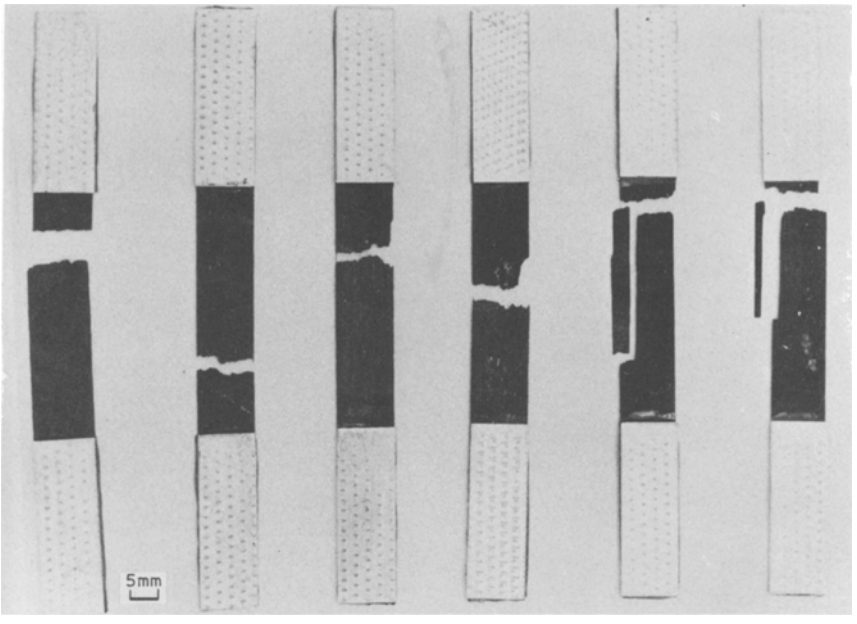

Figure 10 Representative examples of modes of fracture found with the fully cured CFRP samples.

cured samples tested in this study showed clear evidence of this type of behaviour in their failure mode. The presence of a stiff matrix that would allow shear stress transfer must modify the failure manner, however, and the examples of broken specimens of fully-cured CFRP in Fig. 10 show that they fractured in a completely different way. All samples broke suddenly in a brittle manner, some yielding two separate peices and others breaking into several fragments. Some of the complex fractures can be explained in terms of secondary failure induced by the shock of rapid elastic recovery after initial failure. But since about half of the test samples simply broke into two pieces the possibility of random damage throughout the specimen should also be considered.

7. Microscopic examination

In order to obtain further information about failure mechanisms in CFRP the specimens have been examined both optically and by scanning electron microscopy. The condition of fibres in the surface layers of broken CFRP specimens was examined by removing the surface layers of matrix with sulphuric acid. Damage to the exposed surface fibres could then be clearly observed under the microscope.

In all specimens, successions of fibre breaks have been found that were not necessarily associated with the final site of complete failure, although the incidence of this sort of damage was greater near to the final fracture point. In samples which failed at the top of the tensile strength scatter band the incidence of this type of fibre damage was much greater away from the final complete fracture site. As Fig. 11 shows, fractures found in the apparently intact portions of the sample are not at right angles to the fibre alignment and loading direction but often run at angles to that direction. Fig. 11b indicates that several fibres comprising small bundles may fail simultaneously at a particular point and that a final shear failure links neighbouring bundle failures.

Although little evidence was found for random, single-fibre failure in most of the samples, such fractures were found in the stronger specimens. Such fractures are shown in Fig. 12. The absence of single fibre breaks in weaker samples probably reflects their comparative rarity rather than their complete absence.

8. Discussion

The acoustic emission patterns obtained from cured CFRP specimens clearly indicate that during tensile loading internal damage is occurring which is similar in nature to that occurring in geometrically identical specimens from which the resin matrix has been removed. Phoenix [11] has shown that the stress–strain behaviour of fibre bundle specimens such as these can be uniquely

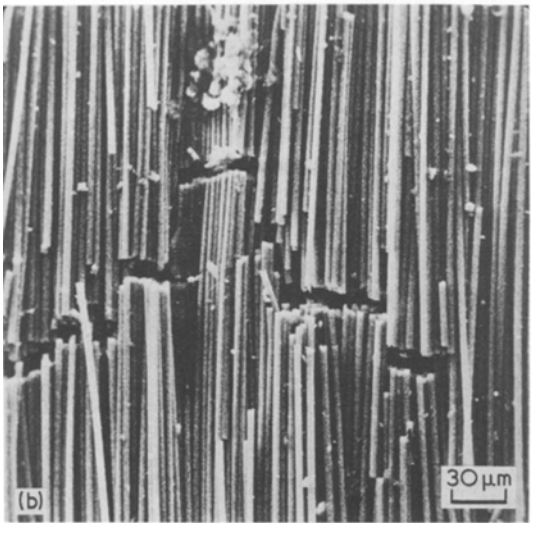

Figure 11 (a) Detail of a fracture found in an apparently intact part of a broken cured CFRP specimen. Note that the fracture is not normal to the direction of fibre alignment. (b) Detail of a fracture which shows that groups of fibres have failed in an associated manner and that individual sub-bundle failures have been linked by shearing parallel to the fibres.

explained in terms of a distribution of fibre strengths combined with a distribution of fibre lengths (range of slackness) in the bundle. The failure of a single fibre in a bundle having no twist results in the load carrying capacity of that fibre being transferred to the other intact fibres in the bundle over the whole bundle length. This is not the case in a composite where there is a relatively rigid matrix capable of transferring stresses by shear between fibres, as discussed by Kelly [12] and others. In such materials the build up in stress over the critical length means that the effect of a

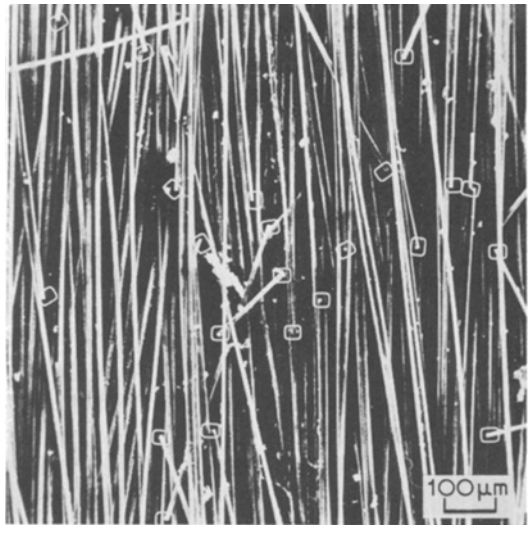

Figure 12 Separate fibre fractures found in an apparently intact region of a broken CFRP specimen.

single fibre fracture is confined to a restricted band of cross-section through the specimen. Within this band the probability of other fibre failures occurring is slightly increased as a result of the overall rise in stress. The width of this band has been arbitrarily taken by Rosen to be that distance from the fibre fracture end at which the stress in the fibre is 90% of the stress which would be carried by an unbroken fibre [5]. The distribution of faults along fibres will mean, however, that successive failures of fibres in the composite will not necessarily occur in this cross-section. This picture of accumulation of fibre damage leading to a general weakening of the specimen and eventual failure when sufficient fibre failures have occurred in a particular cross-sectional band is described in more detail by Zweben and Rosen [13]. The model considers that the broken fibres which lead to the ultimate weakening of one cross-section are not necessarily adjacent but are likely to be so because of stress concentration effects. Our Fig. 11a and b shows that adjacent fracture does occur, although it is apparently confined to sub-bundles containing only a few fibres. The observation made in an earlier paper [8] that these samples showed no evidence of notch sensitivity and that an acoustic emission study indicated blunting by shear failure may mean that these associated fibre failures are limited by shear failure between sub-bundles.

The linear elastic fracture mechanics model which treats CFRP as an anisotropic, homogeneous material implies the development of a

single flaw of critical size, with its characteristic stress concentration, followed by complete failure of crack propagation through successive adjacent regions of fibres and matrix. However, a comparison of the AE results obtained from bundle and semi-cured specimens, together with the microscopic examination of failed CFRP specimens leads us to conclude that the basic mechanisms of failure are statistically determined and are not a result of straightforward crack propagation. Successive fibre failure, i.e. conventional crack propagation, certainly does occur but it appears to be localized and results in a distribution of weak regions in the specimen.

The greater number of acoustic emissions and the evidence of widely-distributed fibre damage in specimens at the top of the tensile strength scatter band suggest that the scatter in the strength of composites is not merely a result of poor manufacture but is an inherent characteristic. The variation in breaking strains of CFRP specimens can be seen from Fig. 3 to span the strain range from the point at which both acoustic emissions and the change of slope of the σ/ϵ curve for bundle and semi-cured specimens indicate that a significant number of fibres are failing, at a maximum strain just greater than that reached by any of the bundles. This suggests that those samples near the bottom of the scatter band failed because of a chance accumulation of weak regions in a given cross-section. The upper limit of the scatter band would be defined by specimens in which the points of weakness chanced to be more nearly randomly-distributed through the specimen so that the cross-sectional bands were able to sustain higher loads.

9. Conclusion

While the mode of fracture of cured, unidirectional CFRP specimens is very different from those of semi-cured and bundle specimens, the acoustic emissions and internal deformation processes which occur during tensile loading are closely related to the basic fibre bundle structure. The difference in failure mode can be attributed to the role played by the matrix in stress transfer between broken and intact fibres which ensures that a failed fibre can continue to contribute to the load-carrying capacity of the specimen. The frequency of failure of CFRP specimens was found to be related to the strain range over which fibres failed in the bundle specimens although approximately 10% of the CFRP specimens exceeded the maximum strain reached by the bundles. This leads us to conclude that although microscopic examination reveals crack growth in sub-bundles of fibres, this is limited, at least initially, by shearing between these sub-bundles and eventual failure is attributable to the statistically-determined accumulation of fracture regions across a particular cross-section. This also indicates that the scatter in the strength of composite materials is not entirely due to manufacturing faults but is an inherent characteristic of the material.

Acknowledgements

The authors are grateful to the Science Research Council and to the Mitsubishi Petrochemical Co for financial support. We would like to acknowledge several stimulating discussions with Dr D. E. W. Stone, of R.A.E., Farnborough.

References

1. D. C. PHILLIPS, *J. Comp. Mat.* **8** (1974) 130.
2. B. HARRIS, P. W. R. BEAUMONT and E. MONCUNILL DE FERRAN, *J. Mater. Sci.* **6** (1971) 238.
3. P. W. R. BEAUMONT and B. HARRIS, *ibid,* **7** (1972) 1265.
4. M. E. WADDOUPS, J. R. EISENMANN and B. E. KAMINSKI, *ibid* **5** (1971) 446.
5. B. W. ROSEN, *AIAAJ* **2** (1964) 1985.
6. C. ZWEBEN, *Comp. Mat. Testing & Design,* ASTM STP 460 (1969) 528.
7. R. B. MCKEE and G. SINES, *J. Elastoplastics* **1** (1969) 185.
8. M. FUWA, A. R. BUNSELL and B. HARRIS, to be published.
9. Courtaulds Grafil data sheets.
10. H. L. DUNEGAN and A. T. GREEN, *Mat. Res. Stand.* **11** (1971) 3.
11. S. L. PHOENIX, *Fibre Sci. Tech.* **7** (1974) 15.
12. A. KELLY, "Strong Solids" (Clarendon Press, Oxford, 1966).
13. C. ZWEBEN and B. W. ROSEN, *J. Mech. Phys. Solids* **18** (1970) 189.

Received 22 April and accepted 20 May 1975.